



## OPEN ACCESS

## EDITED BY

Mary Byrne,  
The University of Sydney, Australia

## REVIEWED BY

Alfredo Cruz-Ramirez,  
National Polytechnic Institute of Mexico  
(CINVESTAV), Mexico  
Hiroyasu Motose,  
Okayama University,  
Japan

## \*CORRESPONDENCE

Markus G. Stetter  
m.stetter@uni-koeln.de  
Martin Hülskamp  
martin.huelskamp@uni-koeln.de

## SPECIALTY SECTION

This article was submitted to  
Plant Development and EvoDevo,  
a section of the journal  
Frontiers in Plant Science

RECEIVED 07 April 2022

ACCEPTED 24 August 2022

PUBLISHED 23 September 2022

## CITATION

Koebke E, Stephan L, Stetter MG and  
Hülskamp M (2022) Functional analysis of  
the BEige and Chediak-Higashi domain  
gene MpSPIRRIG in *Marchantia*  
*polymorpha*.  
*Front. Plant Sci.* 13:915268.  
doi: 10.3389/fpls.2022.915268

## COPYRIGHT

© 2022 Koebke, Stephan, Stetter and  
Hülskamp. This is an open-access article  
distributed under the terms of the [Creative  
Commons Attribution License \(CC BY\)](#). The  
use, distribution or reproduction in other  
forums is permitted, provided the original  
author(s) and the copyright owner(s) are  
credited and that the original publication in  
this journal is cited, in accordance with  
accepted academic practice. No use,  
distribution or reproduction is permitted  
which does not comply with these terms.

# Functional analysis of the BEige and Chediak-Higashi domain gene MpSPIRRIG in *Marchantia polymorpha*

Eva Koebke, Lisa Stephan, Markus G. Stetter\* and  
Martin Hülskamp\*

Botanical Institute, University of Cologne, Cologne, Germany

BEige and Chediak-Higashi domain containing proteins (BDCPs) have been described to function in membrane-dependent processes in eukaryotes. This role was also observed for the BDCP SPIRRIG (SPI) in the model plant *Arabidopsis thaliana* in the context of cell morphogenesis. Additionally, *AtSPI* was found to control salt stress resistance by mediating mRNA stability and salt stress-dependent processing body formation. In this work, we utilize an evolutionarily comparative approach to unravel conserved, basal BDCP functions in the liverwort *Marchantia polymorpha*. Our phenotypic and physiological analyses show that MpSPI is involved in cell morphogenesis and salt resistance regulation, indicating that both functions are evolutionarily conserved between the two species. Co-localization was found with endosomal and P-body markers, suggesting links to membrane-dependent processes and mRNA metabolism. Finally, we present transcriptomics data showing that *AtSPI* and MpSPI regulate orthologous genes in *A. thaliana* and *M. polymorpha*.

## KEYWORDS

**SPIRRIG, *Marchantia polymorpha*, BEACH domain protein, salt response, membrane trafficking**

## Introduction

Beige and Chediak-Higashi (BEACH) domain containing proteins (BDCPs) represent a conserved gene family in eukaryotes. BDCPs function as scaffolding proteins in membrane fission and fusion events, including vesicle transport, receptor signaling, apoptosis, and autophagy (Cullinane et al., 2013). Genetic and molecular studies in *A. thaliana* revealed a role in vacuolar and Endosomal Sorting Complex Required for Transport (ESCRT)-mediated membrane trafficking of the BDCP gene *AtSPIRRIG* (*AtSPI*; Saedler et al., 2009; Steffens et al., 2017). *AtSPI* exhibits the classical BDCP domain structure with the characteristic and highly conserved C-terminal end, comprising a pleckstrin homology (PH) domain to bind phospholipids (Cullinane et al., 2013); the BEACH domain, which potentially serves as a ligand-binding site by interacting with the PH domain

(Jogl et al., 2002); and WD40 repeats to mediate protein–protein interactions (Stirnemann et al., 2010).

*Atspi* mutants were initially isolated in an EMS mutagenesis screen due to their weak, distorted trichome phenotype (Hülkamp et al., 1994). Further phenotypic characterization of the mutants revealed *Atspi* to exhibit trichomes with shorter branches and reduced stalk length, less complex epidermal pavement cells, and shorter root hairs and hypocotyls (Saedler et al., 2009). AtSPI has a function in maintaining vacuolar integrity (Saedler et al., 2009) and endosomal transport *via* ESCRT-mediated membrane trafficking through direct interaction with components of the machinery (Steffens et al., 2017). In addition, a role of AtSPI in salt stress-dependent mRNA regulation was uncovered (Steffens et al., 2015): AtSPI interacts with the processing body (P-body) component DECAPPING PROTEIN 1 (AtDCP1) and localizes to and promotes the assembly of P-bodies under salt stress conditions (Steffens et al., 2015). Furthermore, AtSPI was demonstrated to be involved in stabilizing and recruiting salt stress-dependent mRNAs to P-bodies (Steffens et al., 2015). Finally, the finding that mutations in *AtSPI* lead to salt hypersensitivity proved a biologically relevant function of AtSPI in the *A. thaliana* salt stress response (Steffens et al., 2015).

Evolutionary comparison of SPI between *A. thaliana* and *Arabidopsis alpina* demonstrated that the role of SPI in cell morphogenesis and endosomal pathways is conserved between these two Brassicaceae species (Stephan et al., 2021). This is evident from SPI co-localization and interaction with ESCRT components and a similar range of phenotypes. Moreover, a link to P-bodies is suggested by direct protein–protein interaction with P-body markers (Stephan et al., 2021).

In this study, we characterize a *spirrig* T-DNA mutant in the liverwort *Marchantia polymorpha* (*Mpspi*), isolated by Honkanen et al. (2016). During the last decade, *M. polymorpha* has been established as a new molecular model organism to assess comparisons over large evolutionary distances (Mishler and Churchill, 1984; Shimamura, 2016). It enables researchers to study the evolution of land plants, and concomitantly, learn about the basal, minimal genetics coming along with land colonization (Bowman et al., 2007; Ishizaki et al., 2016). The relatively small, fully sequenced genome with a low level of redundancy (Bowman et al., 2017), combined with the dominant, haploid gametophytic life phase of *M. polymorpha*, offers optimal genetic and morphological conditions for reverse and forward genetics. Moreover, *M. polymorpha* can be transformed using *Agrobacterium* (Ishizaki et al., 2008; Kubota et al., 2013), and it is accessible for genome editing *via* homologous recombination (Ishizaki et al., 2013) and CRISPR/Cas9 (Sugano et al., 2014, 2018). Finally, quick and easy tools to analyze the localization, interactions, and functions of proteins of interest, as well as cell morphology, using transient biolistic transformation and staining methods, are available (Westermann et al., 2020).

Here, we present an evolutionarily comparative functional study of *MpSPI*. We show that mutant plants are hypersensitive to salt stress, indicating that the dual role of *AtSPI* in cell

morphogenesis and salt stress response is evolutionarily conserved. In addition, using a comparative RNAseq approach, we present a common set of homologous genes regulated by *A. thaliana* and *M. polymorpha* SPI, strongly suggesting functional conservation of BDCP function between the two species.

## Materials and methods

### Plant materials, growth conditions, and stress treatments

The T-DNA insertion in the *Mpspirrig* mutant (corresponding designations: *Mpspi*-2 and ST17-11; Honkanen et al., 2016) was confirmed by sequencing the amplicon generated with the gene-specific primer 5'-CGAGCCGACTTACCCCTAAT-3' and the T-DNA (pCAMBIA 1300) left border primer 5'-CAGATAAGGGAATTAGGGTTCTATAGG-3'. The male sex of the mutant line was confirmed with the male-specific primer pair 5'-CCAAGTGCGGGCAGAATCAAGT-3' and 5'-TTCATCGCCCGCTATCACCTTC-3', amplifying *rbm27* (Fujisawa et al., 2001).

Plants of the mutant line, the corresponding male ecotype Tak-1, the female ecotype Tak-2, and F1 crossings of Tak-1 and Tak-2 (Tak-1 × Tak-2) were propagated vegetatively under axenic conditions by growing gemmae on Johnson's medium (Johnson et al., 1957) supplemented with 0.8% plant agar under long-day conditions (16h light/8h darkness cycle) and white light (60 μmol m<sup>-2</sup> s<sup>-1</sup>) at 21 ± 2°C.

In order to assess the rhizoid growth, gemmae were grown vertically on solid Johnson's medium without supplements or supplemented with 50 mM NaCl under normal conditions for 7 days.

### Cloning and plasmids

Total RNA was extracted from 14-day-old Tak-1 thalli using TRI reagent (Ambion Life Technologies). RNA was treated with DNaseI (Thermo Scientific) and subjected to oligo(dT)<sub>20</sub> cDNA synthesis using the SuperScript™ III First-Strand cDNA Synthesis Kit (Thermo Scientific). Coding sequences of *MpSPI* PBW (*Mp2g15800*), *MpSPI* PBWF (*Mp2g15800*), *MpLIP5* (*Mp1g06880*), and *MpSKD1* (*Mp8g01610*) were amplified from Tak-1 cDNA (Primer list, Supplementary Table S6). *MpDCP2* (*Mp8g16420*), *MpRAB5*, and *MpARA6* plasmids have been described before (Westermann et al., 2020). *mCH-AtUBP1B* was kindly provided by A. Steffens. *AtKRP1-CFP* was kindly provided by M. Jakoby. Coding sequences were cloned into Gateway vectors pDONR201 and pDONR207 (Invitrogen) and subsequently transferred to respective expression vectors: for localization studies, we used pENSG-YFP/CFP, pEXSG-YFP/CFP (Feys et al., 2005), pAMARENA/pAUBERGINE (M. Jakoby, GenBank ID: FR696418) and pMpGWB406 (Ishizaki et al., 2015); yeast

two-hybrid assays were performed using pAS/pACT (Clontech); and Bimolecular Fluorescence Complementation (BiFC) was performed using pSYN/pSYC (Jakoby et al., 2006) and pCL112/113 (provided by J. F. Uhrig).

## Protein–protein interaction assays

The protocols for yeast two-hybrid assays were described before (Gietz et al., 1995). Positive interactions were selected on plates containing dropout interaction media lacking leucine, tryptophan, and histidine, supplemented with increasing concentrations of 3-Amino-1,2,3-Triazole (3-AT) up to 50 mM. BiFC assays were performed as described previously (Westermann et al., 2020).

## Plant transformation

Transient biolistic transformation of *M. polymorpha* thalli was performed as described before (Westermann et al., 2020). Stable transformation of regenerating *M. polymorpha* thalli fragments with *Agrobacterium tumefaciens* (GV3101 pMP90RK) was conducted as described by Kubota et al. (2013).

## Staining procedures

Fluorescein diacetate (FDA) stainings of young gemmae (5 days old) were performed as described before (Westermann et al., 2020).

## Microscopic analysis

Microscopic observation was carried out with a Leica MZ 16F fluorescence binocular or a Leica TCS SP8 confocal laser scanning microscope using an HC PL APO 20×/0.75 IMM CORR CS2 objective. The excitation and emission of the different fluorophores were performed as described before (Westermann et al., 2020).

## Transcript analysis

Total RNA was extracted from three biological replicates of 14-day-old Tak-1 and *Mpspirrig* thalli grown under normal conditions using TRI reagent (Ambion Life Technologies). RNA integrity was confirmed on a bleach gel (Aranda et al., 2012). 1 µg of DNaseI-treated RNA was subjected to oligo(dT)<sub>20</sub> cDNA synthesis using the SuperScript™ III First-Strand cDNA Synthesis Kit (Thermo Scientific). Quantitative Real-Time PCR (RT-qPCR) was performed in a QuantStudio 5 System (ABI/Life Technologies) using plates (96 well, 0.2 ml) and cover foil (Opti-Seal Optical Disposable Adhesive, BIOplastics) and SYBR

Green reagent (Thermo Fisher Scientific). Subsequent analysis was conducted with the QuantStudio™ Design and Analysis Software version 1.4.1 (ABI/Life Technologies) and Excel 2016. The average of three biological and three technical replicates was calculated. Primer efficiencies were determined using a cDNA dilution series of 1:10, 1:20, 1:40, 1:80, 1:160, and 1:320. Reference gene primers MpADENINE PHOSPHORIBOSYL TRANSFERASE 3 (MpAPT3) and MpACTIN7 (MpACT7) were described before (Saint-Marcoux et al., 2015). The efficiency of the primer pair for MpSPIRRIG (Primer list, supplemental) was accepted with an efficiency of 80–120% and a correlation between –1 and –0.99. Normalization against two reference genes was performed according to the geNorm manual (Vandesompele et al., 2002).

## RNA sequencing and transcriptome analysis

Total RNA for RNAseq analysis was extracted from three biological replicates of 14-day-old Tak-1 and *Mpspirrig* thalli grown under control conditions using TRI reagent (Ambion Life Technologies). Two µg of DNaseI-treated, quality-controlled RNA (RIN > 7, OD<sub>260/280</sub> = 1.8–2.1, OD<sub>260/230</sub> > 1.5) were sent to the Cologne Center for Genomics (CCG) for paired-end 100 bp short-read sequencing. Raw reads were filtered and trimmed using trimmomatic (v 0.39) with SLIDINGWINDOW:4:15 MINLEN:35 LEADING:5 TRAILING:5 (Bolger et al., 2014), and data quality was assessed using MultiQC (v 1.7; Ewels et al., 2016). Filtered reads were aligned to the MpTak1\_v5.1 reference genome (Montgomery et al., 2020) using STAR (v 2.7.3a; Dobin et al., 2013), and reads per gene were counted using the htseq-count function of HTSeq (v 0.11.3; Anders et al., 2015). We further used DESeq2 (v 1.24.0; Love et al., 2014) to compare read counts between Tak-1 and the *Mpspirrig* mutant. We filtered genes for a minimum of ten reads in at least three of the six samples. Differentially expressed genes (DEGs) were filtered using the adjusted value of p cutoff of 0.01 and a log<sub>2</sub> fold change of 1. To test the overlap between DEGs in the *Mpspirrig* mutant and DEGs in *Atspirrig*, we used PhytoMine (v.13)<sup>1</sup> through the intermine (v 1.11.0) Python API to identify homologs between *M. polymorpha* and *A. thaliana* and applied a hypergeometric test for overlap in R. Sequence reads are available on the European Nucleotide Archive under project number PRJEB51622. *M. polymorpha* Gene Ontology (GO) term enrichment analysis was performed as previously described (Busch et al., 2019) with agriGO v.2 (standard settings; <http://systemsbiology.cau.edu.cn/agriGOv2/>; Tian et al., 2017) using gene IDs for the MpTak1\_v3 reference genome.

<sup>1</sup> <https://phytozome-next.jgi.doe.gov/phytomine>

## Results

### The *Marchantia polymorpha* *Mpspi* mutant

The BEACH domain proteins in eukaryotes cluster into four groups (A–D; Saedler et al., 2009) with similar domain structures (Supplementary Figure S1). *AtSPI* belongs to group A and is well conserved throughout the plant kingdom (Supplementary Figure S1; Stephan et al., 2021). Group A members share a Laminin G/Concanavalin A superfamily domain but lack additional domains found in the other groups. BLAST analysis (marchantia.info, MpTak1v5.1) revealed a total of five BDCPs in *M. polymorpha*, and phylogenetic tree construction indicates that *MpSPI* is the closest homolog to *AtSPI* (Supplementary Figure S1).

The overall structure of the *MpSPI* gene is similar to the previously investigated plant *SPI* homologs of *A. thaliana* and *A. alpina*; however, *MpSPI* has an additional FYVE domain downstream of the PBW domain (Figure 1A). FYVE domains are known to target membranes by binding to phosphatidylinositol 3 phosphate (PtdIns(3)P) and are functionally connected to vacuolar protein sorting and endosome function (Gaullier et al., 1998).

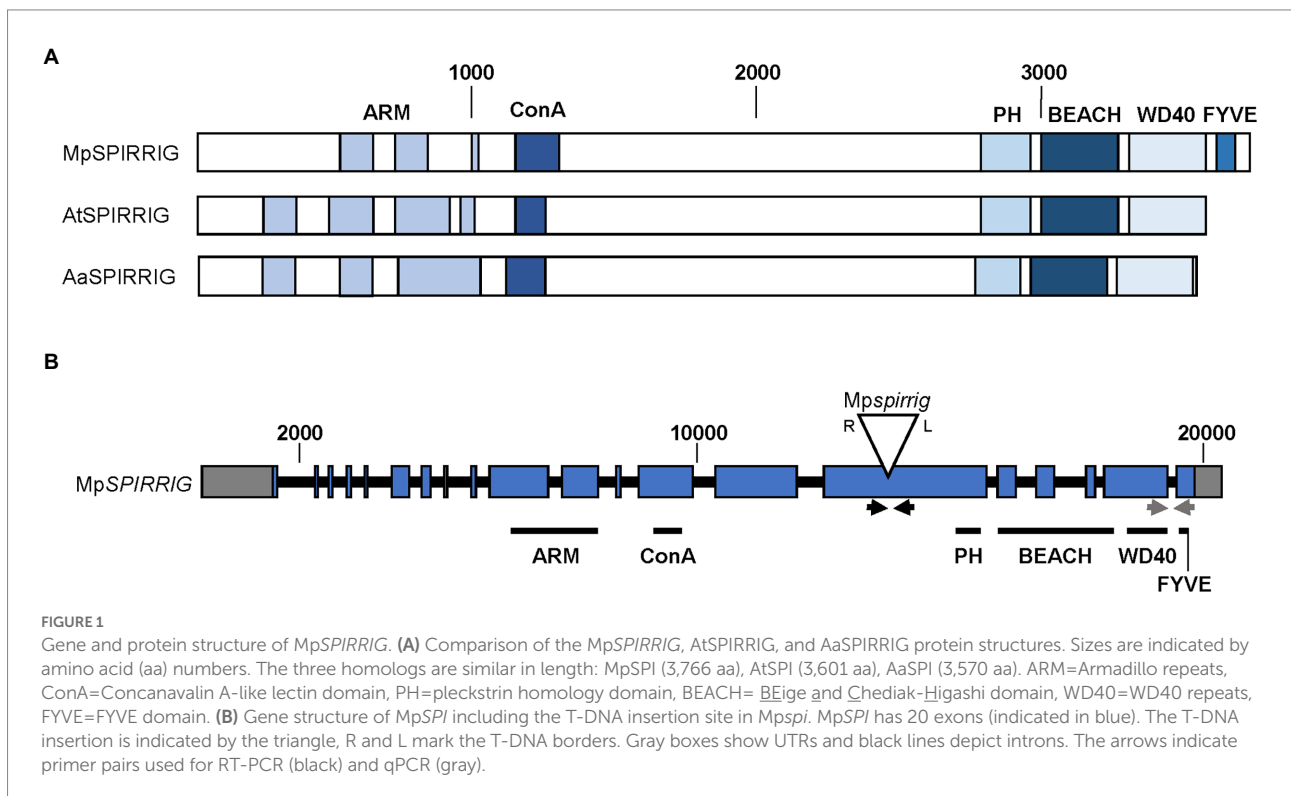
The male T-DNA mutant line *Mpspi*, isolated by Honkanen et al. (2016), harbors a single T-DNA insertion in the 15th exon of *MpSPI* (Honkanen et al., 2016; Figure 1B) upstream of the region

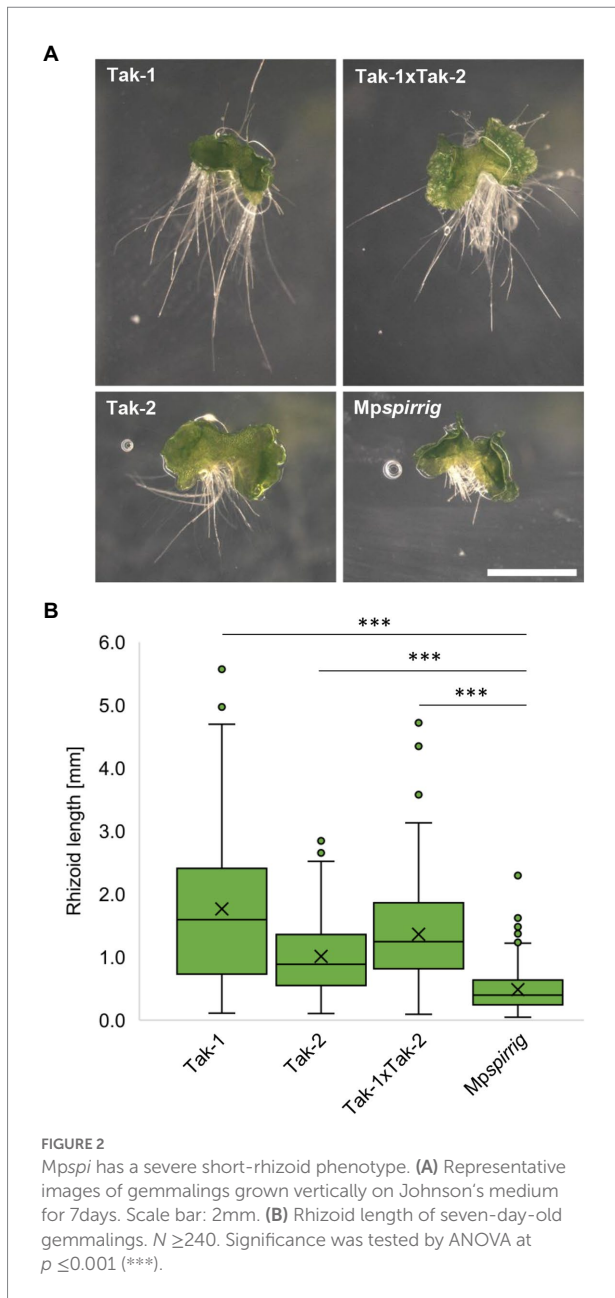
coding for the characteristic C-terminal PBW domain. RT-qPCR experiments using primers located downstream of the insertion site revealed no significant differences between wild type and mutants (Supplementary Figure S2A), indicating that this insertion does not affect the expression levels of *MpSPI*. The produced RNA, however, is incomplete. This is evident from qualitative RT-PCR data, showing that a primer pair spanning the T-DNA insertion site generates no bands in *Mpspi* (Supplementary Figure S2B).

### Morphological phenotypes of *Mpspirrig* gemmae

Honkanen et al. (2016) initially identified *Mpspi* by its short rhizoid phenotype. We confirmed this phenotype in seven-day-old gemmalings. *Mpspi* showed a clear reduction in rhizoid length compared to Tak-1 (3.6 fold), Tak-2 (2.1 fold), and Tak-1xTak-2F1 gemmalings (2.8 fold; Figure 2A). Statistical analysis revealed that this reduction is significant ( $p \leq 0.001$ ; Figure 2B).

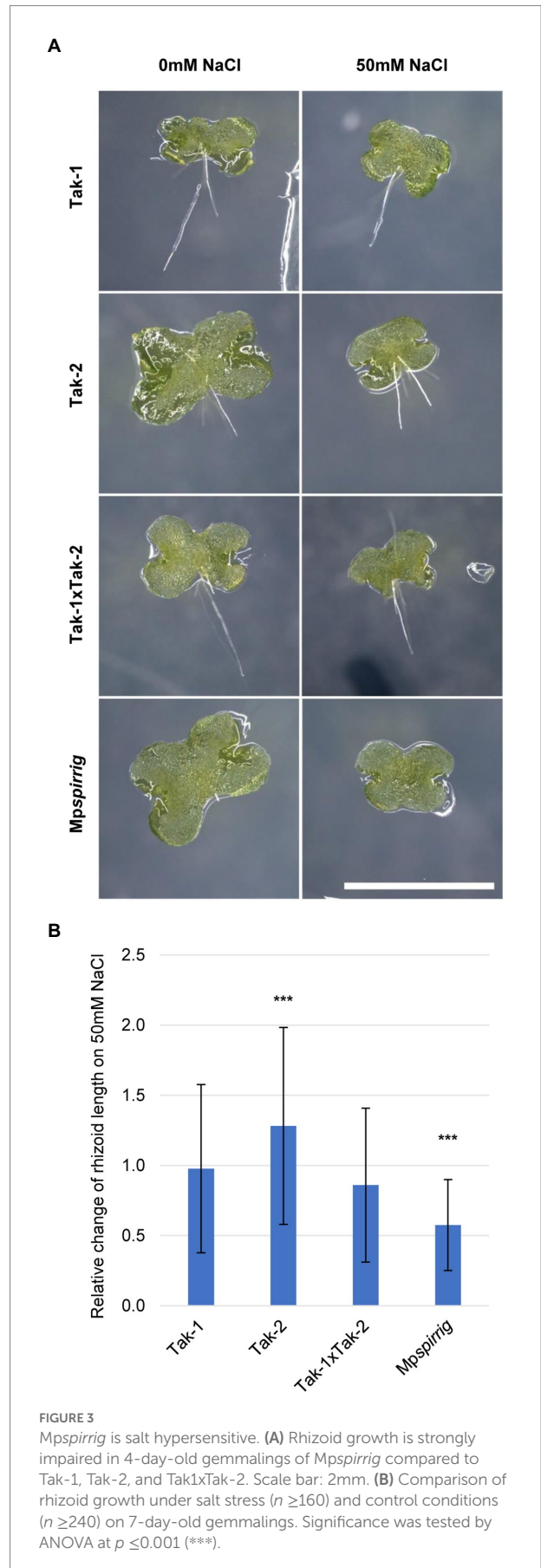
As *Atspi* mutants in Arabidopsis display fragmented vacuoles (Saedler et al., 2009), we stained five-day-old gemmae with fluorescein diacetate (FDA). Vacuoles in rhizoids were indistinguishable between Tak-1, Tak-2, Tak1 x Tak-2 crossings, and *Mpspi* (Supplementary Figure S3), similar as found for *A. alpina spirrig* mutants (Stephan et al., 2021).





### Salt stress phenotype of the Mpspirrig mutant

*A. thaliana* and *A. alpina spirrig* mutants show a hypersensitive response to salt stress. In order to investigate whether MpSPI is involved in the *M. polymorpha* salt stress response, we examined the effect of 50 mM NaCl on the rhizoid length of Mpspirrig. Rhizoid length was analyzed after 7 days. We found a significant reduction of the rhizoid length under salt stress conditions (Figure 3). This indicates that Mpspi is salt hypersensitive and that MpSPI is relevant for the salt stress response in *M. polymorpha*.



## MpSPI interacts with ESCRT components

The association of *A. thaliana* and *A. alpina* SPI with membrane-dependent processes is suggested by co-localization and direct protein–protein interactions with ESCRT components (Steffens et al., 2017; Stephan et al., 2021). To test whether SPI in *M. polymorpha* shares this behavior, we first performed co-localization assays in *M. polymorpha* epidermal cells. Toward this end, we focused on MpSPI, MpLIP5, and MpSKD1, for which co-localization and interactions were reported for *A. thaliana* and *A. alpina* (Steffens et al., 2017; Stephan et al., 2021).

Co-localization experiments were done with protein fragments of MpSPI as we were not able to construct the about 12 kb long full-length CDS. The fragments were chosen to fit Arabidopsis and Arabis fragments used in previous studies to facilitate comparison. MpSPI PBW alone localizes to distinct cytoplasmic dots in transient assays as well as in stably transformed Tak-1 thalli (Figures 4A,E). The localization was neither dependent on the position of the fluorescent tag nor on the presence of the C-terminal FYVE domain (Figures 4B,C). This localization behavior differs from AtSPI to AaSPI, which are evenly distributed in the cytoplasm (Steffens et al., 2017; Stephan et al., 2021). To test whether this is a property of MpSPI or the cellular environment, we studied MpSPI localization in transiently transformed

*A. thaliana* epidermal cells. Here as well, MpSPI was localized to dots indicating that the localization behavior is not primarily triggered by the cellular environment (Figure 4D).

MpLIP5 and MpSKD1 both localize to cytoplasmic, dot-like structures (Figures 5A,B), which co-localize entirely with MpSPI PBW in double transformations (Figures 5C,D). In contrast, co-localization experiments with the endosomal marker proteins MpRas-related in brain 5 (MpRAB5) and MpARA6 (also known as RABF1) revealed only partial overlap supporting a direct interaction of MpSPI with MpLIP5 and MpSKD1, rather than a general localization to endosomal structures (Supplementary Figure S4, S5).

To test this, we assessed direct protein–protein interactions of MpSPI with ESCRT components in pairwise yeast two-hybrid assays. While no interaction between MpSPI PBW/PBWF and MpSKD1 was detectable, we found a strong interaction between MpSPI PBW/PBWF and MpLIP5 (Supplementary Table S1). However, this interaction could not be independently confirmed. Bimolecular fluorescence complementation (BiFC) assays in cells of *M. polymorpha* (Supplementary Figure S6), *A. thaliana*, *A. porrum*, and *N. benthamiana* showed no interactions of MpSPI PBW with MpSKD1 or MpLIP5. Moreover, Förster Resonance Energy Transfer-Acceptor Photobleaching (FRET-AP) and pull-down assays experimentally did not succeed in our hands.

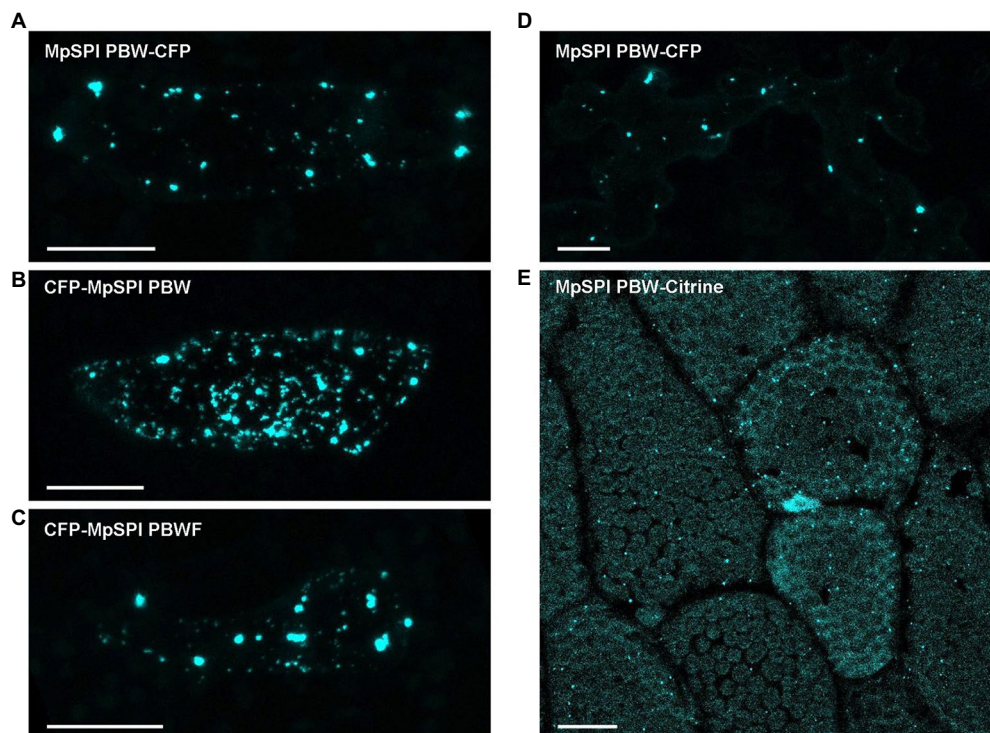


**FIGURE 4**

MpSPI PBW localizes to dot-like structures under non-stress conditions. (A) Transiently expressed, CFP tagged MpSPI PBW localizes to punctate structures in Tak-1 epidermal cells under normal conditions (B) irrespective of the position of the fluorescent tag and (C) the addition of the FYVE domain. Scale bars: 25µm. (D) Transiently expressed, CFP tagged MpSPI PBW localizes to punctate structures in *A. thaliana* Col-0 epidermal cells under normal conditions. Scale bar: 25µm. (E) Citrine tagged MpSPI PBW was stably transformed into regenerating Tak-1 thalli. Image shows a 5-day-old gemmae derived from the stable line. Scale bar: 25µm.

Expressed MpLIP5 was non-specifically bound by any protein tag, and it was not possible to detect MpSPI PBW in protein extracts of a stably transformed *M. polymorpha* line or to simultaneously detect MpSPI PBW and MpLIP5 in protein extracts of transiently transformed *N. benthamiana* leaves by immunoblotting.

## MpSPI localizes to P-bodies

In *A. thaliana*, the PBW domain of SPI localizes to P-bodies under salt stress and differentially regulates the stability of RNAs in this context (Steffens et al., 2015). To test whether this is also the case in *M. polymorpha*, we transiently co-expressed MpDCP2 and MpSPI PBW. We found a strong co-localization in punctate structures under normal conditions (Figure 6A). However, the number of P-bodies labeled by MpSPI PBW was not altered by salt

stress (150 mM NaCl for 60 min; Figures 6A,B). Interestingly, the stress granule marker AtUBP1B, which localizes to dots upon stress in *A. thaliana* (Nguyen et al., 2016), is also present in granules already under non-stress conditions in *M. polymorpha* (Supplementary Figure S7).

To further support an association of MpSPI with P-bodies, we tested protein–protein interactions of MpSPI with MpDCP1. However, we found no interaction in pairwise yeast two-hybrid and BiFC assays in *M. polymorpha*.

## Differentially expressed genes (DEGs) overlap in *Mpspirrig* and *Atspi* mutants

The finding that MpSPI is relevant for morphogenesis and salt stress, similar to *Arabidopsis thaliana* and *Arabidopsis alpina*, raised the

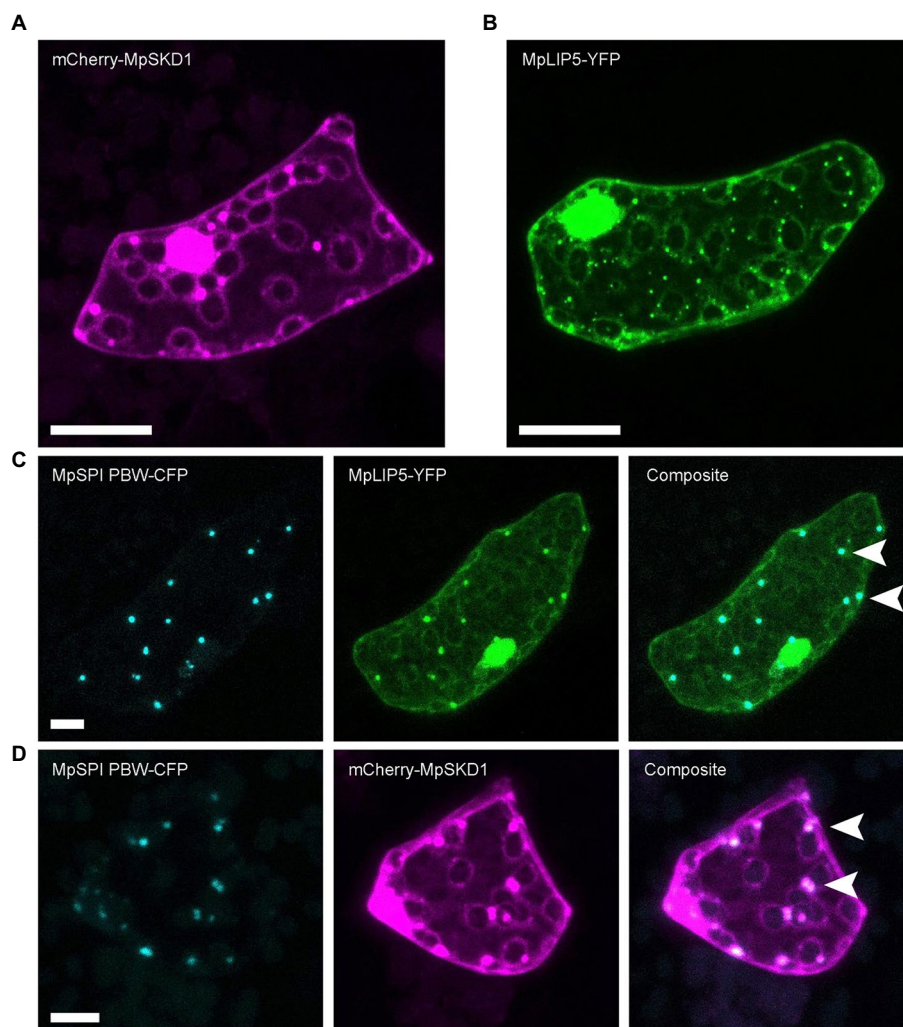
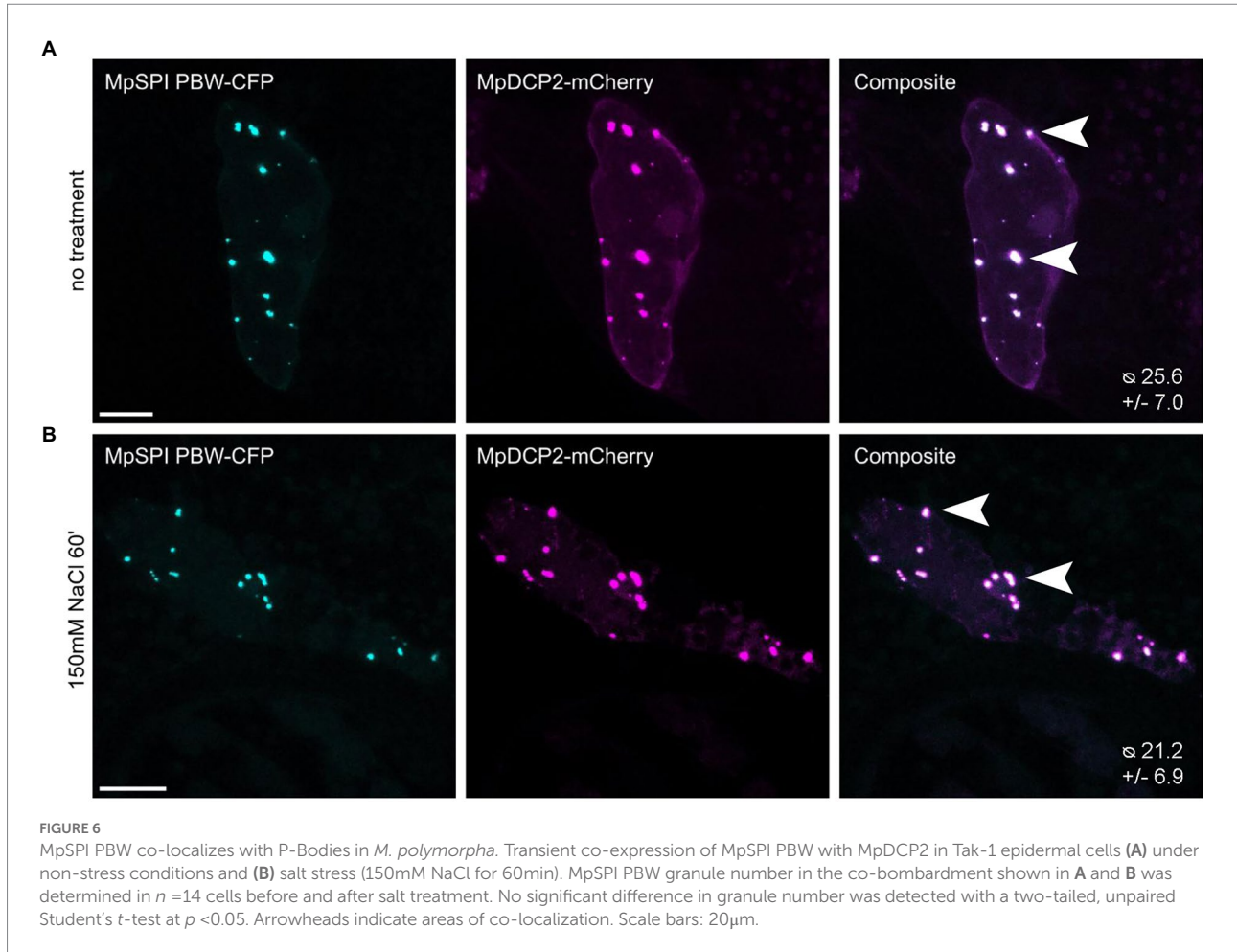


**FIGURE 5**  
MpSPI PBW co-localizes with ESCRT components in *M. polymorpha*. **(A)** Dot-like localization of transiently expressed mCherry-MpSKD1 in Tak-1 epidermal cells. **(B)** Dot-like localization of transiently expressed MpLIP5-YFP in Tak-1 epidermal cells. **(C)** Transient co-expression of MpSPI PBW and MpLIP5-YFP in Tak-1 epidermal cells. **(D)** Transient co-expression of MpSPI PBW and MpSKD1 in Tak-1 epidermal cells. Arrowheads indicate areas of co-localization. Scale bars=20μm.



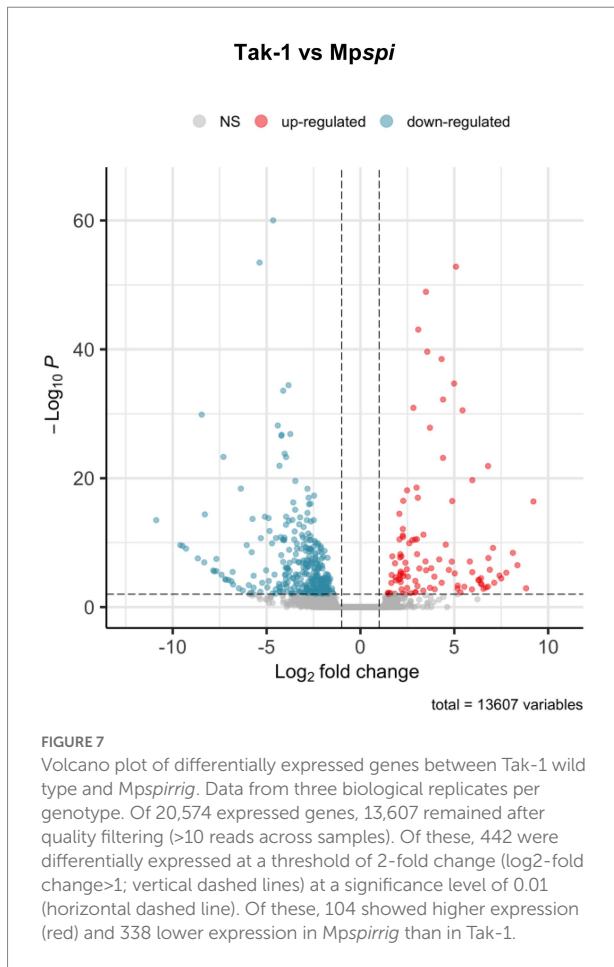
question of whether SPI regulates common downstream genes. Previous experiments have shown that many genes are differentially expressed when comparing wild type and *spi* mutants in *A. thaliana* (Steffens et al., 2015). To explore this, we employed a comparative, genome-wide transcriptome analysis of *Mpspi* and wild type plants. Total RNA of both plant lines was extracted from three biological replicates of 14-day-old plants grown under normal conditions and subjected to RNAseq. All six samples had over 30 million reads each, with at least 19.5 million reads mapping to exonic regions. All samples clustered according to the genotype based on read counts (Supplementary Figure S8). Of the 20,574 expressed genes, 13,607 genes were retained after filtering (minimum ten reads in at least three samples; Figure 7). We identified 442 significantly DEGs ( $p < 0.01$ ), comprising 104 upregulated and 338 downregulated genes, with at least 2-fold expression change between wild type and mutant (Supplementary Figure S9, Figure 7 and Supplementary Table S2). Consistent with our RT-qPCR analysis, the read count of *MpSPI* was not significantly different in *Mpspirrig* samples and the wild type (Supplementary Figure S10).

To determine common involvement in biological processes among the DEGs, we analyzed enriched GO terms (Figure 8). Among 217 *M. polymorpha* genes with annotated terms, we found

a total of 20 significantly enriched GO terms in the category *biological processes* (FDR < 0.05, Figure 8). Interestingly, the six most strongly enriched GO terms oxidation–reduction process, single-organism metabolic process, response to oxidative stress, response to stress, response to stimulus, single-organism process, in that order (FDR < 5E–05, Supplementary Table S3) are present among the most strongly enriched GO terms of significant DEGs in *A. thaliana spirrig* mutants as well (FDR < 5E–05, Supplementary Table S4, derived from RNAseq data of Steffens et al., 2017). Next, we compared the set of significant DEGs (fold change > 2) in *Mpspirrig* to all significant DEGs in *A. thaliana spirrig* mutants (RNAseq data of Steffens et al., 2017). For 127 of the 442 DEGs, we could identify an *A. thaliana* ortholog using PhytoMine. Finally, we found a highly significant overlap ( $p = 4.08e-10$ ) of 20 DEGs between *Mpspirrig* and *Atspirrig* (Supplementary Table S5).

## Discussion

In this work we studied the molecular and biological function of *MpSPI* in the liverwort *Marchantia polymorpha* to enable an evolutionary comparison with two other plant species in which



the homolog gene was characterized, *Arabidopsis thaliana* and *Arabis alpina*.

## Is MpSPI a homolog of the *Arabidopsis* SPI gene?

We consider MpSPI as an AtSPI homolog based on the finding that it clusters in the same group in a phylogenetic tree considering the BEACH domain (Supplementary Figure S1). MpSPI differs, however, from BDCPs in angiosperms at the structural level as it exhibits a FYVE domain in the C-terminus. FYVE domains target membranes by binding to phosphatidylinositol 3 phosphate (PtdIns(3)P; Gaullier et al., 1998). Both the human BDCP HsWDFY3/autophagy-linked FYVE protein (ALFY) and its *Drosophila* ortholog Blue cheese (Bchs) carry a FYVE domain downstream of the PBW domain and are involved in the clearance of aggregated proteins for autophagic degradation. In *A. thaliana*, none of the BDCP family members exhibit a FYVE domain (Teh et al., 2015). Recently, Agudelo-Romero et al. (2020) argued that the FYVE domain has been lost during land plant evolution because it has lost its essential function. This is consistent with our finding that protein fragments with and without the FYVE domain showed the same localization behavior. However, a more

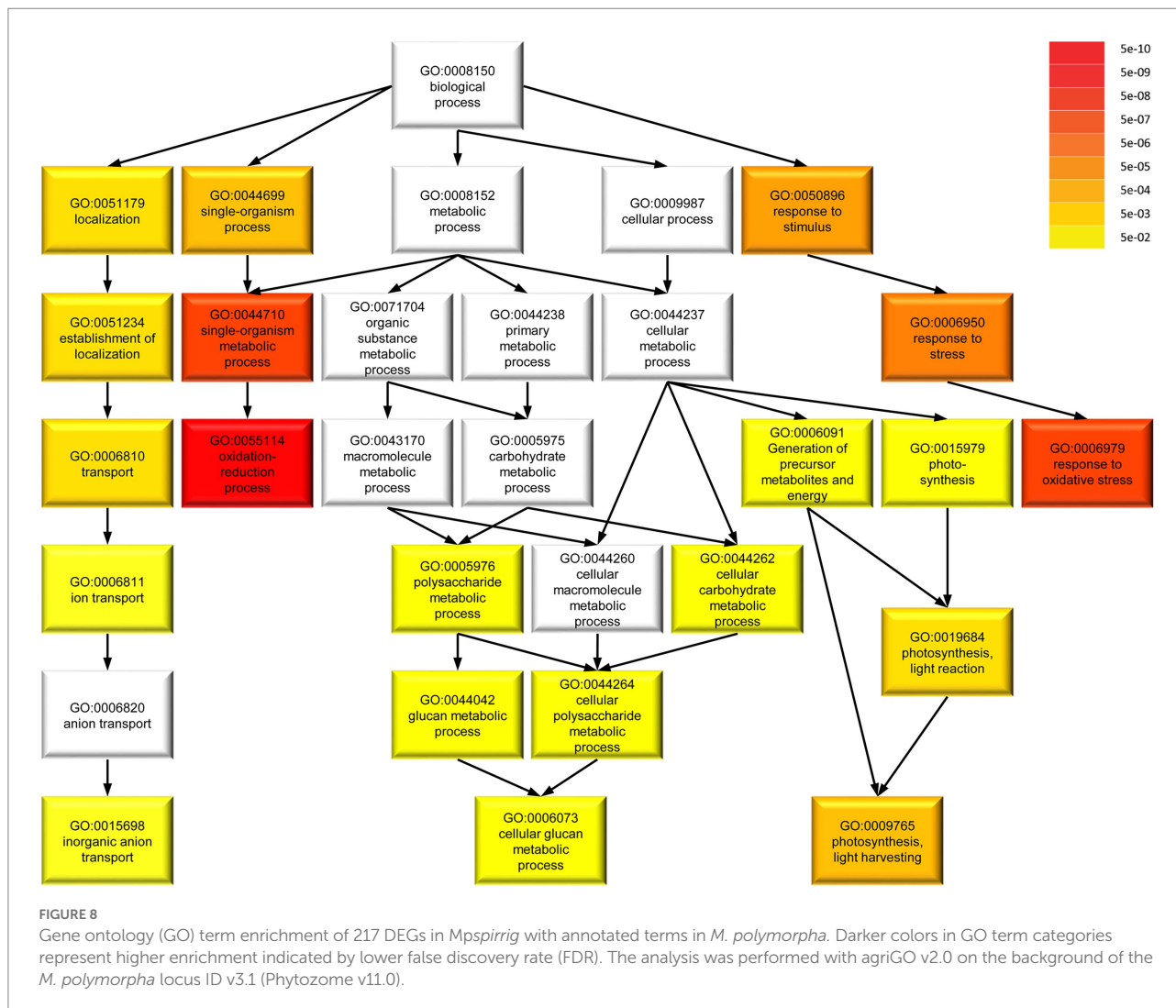
detailed molecular analysis would be necessary to explore this question.

## The dual role of SPI in morphogenesis and salt resistance is evolutionary conserved

The *Arabidopsis* SPI gene has been described to be important in two processes that appear to be unrelated: cell morphogenesis and salt resistance (Steffens et al., 2015). The finding that a second, evolutionary distant Brassicaceae species, *Arabis alpina*, shows similar phenotypes in both processes suggested that the dual function is evolutionary conserved within that family (Stephan et al., 2021). The data reported in this study suggest that also MpSPI in *Marchantia polymorpha* is involved in both processes. We found a clear hypersensitive response to salt stress. The role of MpSPI in cell morphogenesis is evident from the short root hair phenotype. While the latter was reported in two independent alleles, we could only analyze one allele with respect to its response to salt stress. Our attempts to generate a second allele by CRISPR or to rescue the mutant phenotype failed for technical reasons. Therefore, we cannot exclude that the salt stress phenotype is due to a background mutation.

## The association of SPI with endosomal structures and P-bodies is evolutionary conserved

The molecular analysis of SPI in *A. thaliana* has revealed the co-localization of SPI protein with endosomes and P-bodies (Steffens et al., 2015, 2017). In addition, physical interactions of SPI with canonical endosomal proteins such as LIP5 and SKD1 and the P-body protein DCP1 were found suggesting that SPI exerts a molecular function in the two compartments (Steffens et al., 2015, 2017). We found no convincing evidence supporting the direct interaction of MpSPI with the interactors found in *Arabidopsis*. However, co-localization experiments with MpSPI revealed clear association with MpSKD1 and MpLIP5. This co-localization appears to be specific to a subpopulation of endosomes as the endosomal marker MpARA6 and MpRAB5 revealed only partial co-localization. This selective binding to MpSKD1 and MpLIP5 labeled endosomes may reflect a functional link. This may occur through MpLIP5 for which we found an interaction in yeast two-hybrid assays. Similarly, the co-localization of MpSPI with the P-body marker MpDCP2 may reflect a functional association, though the molecular basis remains elusive without the identification of an interaction partner. It is interesting to note, that in contrast to *Arabidopsis*, the association of MpSPI to P-bodies is not stress-dependent. Given that also the stress granule marker is associated in granules under non-stress conditions, it is likely that P-bodies and stress granules are constitutively present.



## Mpspi regulates stress response genes and a common set of genes also regulated by *Arabidopsis* SPI

Our genome-wide transcriptome comparison of *Mpspi* and wild-type revealed 442 significant DEGs with at least 2-fold change in expression. Our analysis revealed several strongly enriched GO terms that all suggest a role in stress responses. Strikingly, the significantly enriched GO terms in *Arabidopsis* are very similar suggesting that the transcriptional changes in *spi* mutants affect the stress response machinery in both species. We extended this analysis aiming to identify specific genes that are differentially regulated by both species in a SPI-dependent manner. Out of the 442 DEGs in *Marchantia* we could identify 127 orthologs out of which 20 DEGs were shared by *Marchantia* and *Arabidopsis*. While these genes do not immediately suggest the regulation of specific biological pathways, it is remarkable that 20 orthologous genes are regulated by SPI despite the enormous evolutionary distance.

## Data availability statement

The data presented in the study are deposited in the European Nucleotide Archive repository, accession number PRJEB51622.

## Author contributions

EK, LS, and MH designed this study. EK, LS, MS, and MH wrote the manuscript. EK and LS performed the research. EK, LS, and MS analyzed the data. All authors contributed to the article and approved the submitted version.

## Funding

This work was supported by the Deutsche Forschungsgemeinschaft Grant HU 497/15-1 (MH).

## Acknowledgments

We thank Liam Dolan for providing the wild-type and *Mpspirrig* mutant lines, and Hyung-Woo Jeon for providing F1 spores from crossings of Tak-1 and Tak-2. We also thank Roswitha Lentz for excellent technical assistance and Timothy Jobe and Aurélien Boisson-Dernier for very helpful discussions.

## Conflict of interest

The authors declare that the research was conducted in the absence of any commercial or financial relationships that could be construed as a potential conflict of interest.

## References

- Agudelo-Romero, P., Fortes, A. M., Suárez, T., Lascano, H. R., and Saavedra, L. (2020). Evolutionary insights into FYVE and PHOX effector proteins from the moss *Physcomitrella patens*. *Planta* 251, 1–20. doi: 10.1007/s00425-020-03354-w
- Anders, S., Pyl, P. T., and Huber, W. (2015). HTSeq—a python framework to work with high-throughput sequencing data. *Bioinformatics* 31, 166–169. doi: 10.1093/bioinformatics/btu638
- Aranda, P. S., LaJoie, D. M., and Jorcyk, C. L. (2012). Bleach gel: a simple agarose gel for analyzing RNA quality. *Electrophoresis* 33, 366–369. doi: 10.1002/elps.201100335
- Bolger, A. M., Lohse, M., and Usadel, B. (2014). Trimmomatic: a flexible trimmer for Illumina sequence data. *Bioinformatics* 30, 2114–2120. doi: 10.1093/bioinformatics/btu170
- Bowman, J. L., Floyd, S. K., and Sakakibara, K. (2007). Green genes-comparative genomics of the green branch of life. *Cells* 129, 229–234. doi: 10.1016/j.cell.2007.04.004
- Bowman, J. L., Kohchi, T., Yamato, K. T., Jenkins, J., Shu, S., Ishizaki, K., et al. (2017). Insights into land plant evolution garnered from the *Marchantia polymorpha* genome. *Cells* 171, 287–304.e15. doi: 10.1016/j.cell.2017.09.030
- Busch, A., Deckena, M., Almeida-Trapp, M., Kopischke, S., Kock, C., Schüssler, E., et al. (2019). MpTCP1 controls cell proliferation and redox processes in *Marchantia polymorpha*. *New Phytol.* 224, 1627–1641. doi: 10.1111/nph.16132
- Cullinane, A. R., Schäffer, A. A., and Huizing, M. (2013). The BEACH is hot: a LYST of emerging roles for BEACH-domain containing proteins in human disease. *Traffic* 14, 749–766. doi: 10.1111/tra.12069
- Dobin, A., Davis, C. A., Schlesinger, F., Drenkow, J., Zaleski, C., Jha, S., et al. (2013). STAR: ultrafast universal RNA-seq aligner. *Bioinformatics* 29, 15–21. doi: 10.1093/bioinformatics/bts635
- Ewels, P., Magnusson, M., Lundin, S., and Käller, M. (2016). MultiQC: summarize analysis results for multiple tools and samples in a single report. *Bioinformatics* 32, 3047–3048. doi: 10.1093/bioinformatics/btw354
- Feys, B. J., Wiermer, M., Bhat, R. A., Moisan, L. J., Medina-Escobar, N., Neu, C., et al. (2005). Arabidopsis SENESCENCE-ASSOCIATED GENE101 stabilizes and signals within an ENHANCED DISEASE SUSCEPTIBILITY1 complex in plant innate immunity. *Plant Cell* 17, 2601–2613. doi: 10.1105/tpc.105.033910
- Fujisawa, M., Hayashi, K., Nishio, T., Bando, T., Okada, S., Yamato, K. T., et al. (2001). Isolation of X and Y chromosome-specific DNA markers from a liverwort, *Marchantia polymorpha*, by representational difference analysis. *Genetics* 159, 981–985. doi: 10.1093/genetics/159.3.981
- Gaullier, J.-M., Simonsen, A., D'Arrigo, A., Bremnes, B., and Stenmark, H. (1998). FYVE finger proteins as effectors of phosphatidylinositol 3-phosphate. *Chem. Phys. Lipids* 98, 87–94. doi: 10.1016/S0009-3084(99)00021-3
- Gietz, R. D., Schiestl, R. H., Willems, A. R., and Woods, R. A. (1995). Studies on the transformation of intact yeast cells by the LiAc/SS-DNA/PEG procedure. *Yeast* 11, 355–360. doi: 10.1002/yea.320110408
- Honkanen, S., Jones, V. A. S., Morier, G., Champion, C., Hetherington, A. J., Kelly, S., et al. (2016). The mechanism forming the cell surface of tip-growing rooting cells is conserved among land plants. *Curr. Biol.* 26, 3238–3244. doi: 10.1016/j.cub.2016.09.062
- Hülkamp, M., Misra, S., and Jürgens, G. (1994). Genetic dissection of trichome cell development in *Arabidopsis*. *Cells* 76, 555–566. doi: 10.1016/0092-8674(94)90118-X
- Ishizaki, K., Chiyoda, S., Yamato, K. T., and Kohchi, T. (2008). Agrobacterium-mediated transformation of the haploid liverwort *Marchantia polymorpha* L., an emerging model for plant biology. *Plant Cell Physiol.* 49, 1084–1091. doi: 10.1093/pcp/pcn085
- Ishizaki, K., Johzuka-Hisatomi, Y., Ishida, S., Iida, S., and Kohchi, T. (2013). Homologous recombination-mediated gene targeting in the liverwort *Marchantia polymorpha* L. *Sci. Rep.* 3, 1–6. doi: 10.1038/srep01532
- Ishizaki, K., Nishihama, R., Ueda, M., Inoue, K., Ishida, S., Nishimura, Y., et al. (2015). Development of gateway binary vector series with four different selection markers for the liverwort *Marchantia polymorpha*. *PLoS One* 10, 1–13. doi: 10.1371/journal.pone.0138876
- Ishizaki, K., Nishihama, R., Yamato, K. T., and Kohchi, T. (2016). Molecular genetic tools and techniques for *Marchantia polymorpha* research. *Plant Cell Physiol.* 57, 262–270. doi: 10.1093/pcp/pcv097
- Jakoby, M. J., Weinl, C., Pusch, S., Kuijt, S. J. H., Merkle, T., Dissmeyer, N., et al. (2006). Analysis of the subcellular localization, function, and proteolytic control of the Arabidopsis cyclin-dependent kinase inhibitor ICK1/KRP1. *Plant Physiol.* 141, 1293–1305. doi: 10.1104/pp.106.081406
- Jogl, G., Shen, Y., Gebauer, D., Li, J., Wiegmann, K., Kashkar, H., et al. (2002). Crystal structure of the BEACH domain reveals an unusual fold and extensive association with a novel PH domain. *EMBO J.* 21, 4785–4795. doi: 10.1093/emboj/cdf502
- Johnson, C. M., Stout, P. R., Broyer, T. C., and Carlton, A. B. (1957). Comparative chlorine requirements of different plant species. *Plant Soil* 8, 337–353. doi: 10.1007/BF01666323
- Kubota, A., Ishizaki, K., Hosaka, M., and Kohchi, T. (2013). Efficient agrobacterium-mediated transformation of the liverwort *Marchantia polymorpha* using regenerating thalli. *Biosci. Biotechnol. Biochem.* 77, 167–172. doi: 10.1271/bbb.120700
- Love, M. I., Huber, W., and Anders, S. (2014). Moderated estimation of fold change and dispersion for RNA-seq data with DESeq2. *Genome Biol.* 15:550. doi: 10.1186/s13059-014-0550-8
- Mishler, B. D., and Churchill, S. P. (1984). A cladistic approach to the phylogeny of the bryophytes. *Brittonia* 36, 406–424. doi: 10.2307/2806602
- Montgomery, S. A., Tanizawa, Y., Galik, B., Wang, N., Ito, T., Mochizuki, T., et al. (2020). Chromatin Organization in Early Land Plants Reveals an ancestral association between H3K27me3, transposons, and constitutive heterochromatin. *Curr. Biol.* 30, 573–588.e7. doi: 10.1016/j.cub.2019.12.015
- Nguyen, C. C., Nakaminami, K., Matsui, A., Kobayashi, S., Kurihara, Y., Toyooka, K., et al. (2016). Oligouridylylate binding protein 1b plays an integral role in plant heat stress tolerance. *Front. Plant Sci.* 7:853. doi: 10.3389/fpls.2016.00853
- Saedler, R., Jakoby, M., Marin, B., Galiana-Jaime, E., and Hülkamp, M. (2009). The cell morphogenesis gene SPIRRIG in *Arabidopsis* encodes a WD/BEACH domain protein. *Plant J.* 59, 612–621. doi: 10.1111/j.1365-313X.2009.03900.x

## Publisher's note

All claims expressed in this article are solely those of the authors and do not necessarily represent those of their affiliated organizations, or those of the publisher, the editors and the reviewers. Any product that may be evaluated in this article, or claim that may be made by its manufacturer, is not guaranteed or endorsed by the publisher.

## Supplementary material

The Supplementary material for this article can be found online at: <https://www.frontiersin.org/articles/10.3389/fpls.2022.915268/full#supplementary-material>

- Saint-Marcoux, D., Proust, H., Dolan, L., and Langdale, J. A. (2015). Identification of reference genes for real-time quantitative PCR experiments in the liverwort *Marchantia polymorpha*. *PLoS One* 10, 1–14. doi: 10.1371/journal.pone.0118678
- Shimamura, M. (2016). *Marchantia polymorpha*: taxonomy, phylogeny and morphology of a model system. *Plant Cell Physiol.* 57, 230–256. doi: 10.1093/pcp/pcv192
- Steffens, A., Bräutigam, A., Jakoby, M., and Hülskamp, M. (2015). The BEACH domain protein SPIRRIG is essential for Arabidopsis salt stress tolerance and functions as a regulator of transcript stabilization and localization. *PLoS Biol.* 13:e1002188. doi: 10.1371/journal.pbio.1002188
- Steffens, A., Jakoby, M., and Hülskamp, M. (2017). Physical, functional and genetic interactions between the Beach domain protein SPIRRIG and LIP5 and SKD1 and its role in Endosomal trafficking to the vacuole in Arabidopsis. *Front. Plant Sci.* 8:1969. doi: 10.3389/fpls.2017.01969
- Stephan, L., Jakoby, M., and Hülskamp, M. (2021). Evolutionary comparison of the developmental/physiological phenotype and the molecular behavior of SPIRRIG between *Arabidopsis thaliana* and *Arabis alpina*. *Front. Plant Sci.* 11:596065. doi: 10.3389/fpls.2020.596065
- Stirnemann, C. U., Petsalaki, E., Russell, R. B., and Müller, C. W. (2010). WD40 proteins propel cellular networks. *Trends Biochem. Sci.* 35, 565–574. doi: 10.1016/j.tibs.2010.04.003
- Sugano, S. S., Nishihama, R., Shirakawa, M., Takagi, J., Matsuda, Y., Ishida, S., et al. (2018). Efficient CRISPR/Cas 9-based genome editing and its application to conditional genetic analysis in *Marchantia polymorpha*. *PLoS One* 13, 1–22. doi: 10.1371/journal.pone.0205117
- Sugano, S. S., Shirakawa, M., Takagi, J., Matsuda, Y., Shimada, T., Hara-Nishimura, I., et al. (2014). CRISPR/Cas 9-mediated targeted mutagenesis in the liverwort *Marchantia polymorpha* L. *Plant Cell Physiol.* 55, 475–481. doi: 10.1093/pcp/pcu014
- Teh, O. K., Hatsugai, N., Tamura, K., Fuji, K., Tabata, R., Yamaguchi, K., et al. (2015). BEACH-domain proteins act together in a cascade to mediate vacuolar protein trafficking and disease resistance in Arabidopsis. *Mol. Plant* 8, 389–398. doi: 10.1016/j.molp.2014.11.015
- Tian, T., Liu, Y., Yan, H., You, Q., Yi, X., Du, Z., et al. (2017). Agri GO v2.0: a GO analysis toolkit for the agricultural community, 2017 update. *Nucleic Acids Res.* 45, W122–W129. doi: 10.1093/nar/gkx382
- Vandesompele, J., De Preter, K., Pattyn, F., Poppe, B., Van Roy, N., De Paepe, A., et al. (2002). The multifunctional FUS, EWS and TAF15 proto-oncoproteins show cell type-specific expression patterns and involvement in cell spreading and stress response. *Genome Biol.* 3:37. doi: 10.1186/gb-2002-3-7-research0034
- Westermann, J., Koebke, R., Lentz, R., Hülskamp, M., and Boisson-Dernier, A. (2020). A comprehensive toolkit for quick and easy visualization of marker proteins, protein–protein interactions and cell morphology in *Marchantia polymorpha*. *Front. Plant Sci.* 11:569194. doi: 10.3389/fpls.2020.569194